Progress In Electromagnetics Research M, Vol. 80, 35–43, 2019

A Slotted UWB Antipodal Vivaldi Antenna for Microwave Imaging Applications

Nurul S. Hasim[1], Kismet A. H. Ping[1, *], Mohammad T. Islam[2], Md. Z. Mahmud[2], Shafrida Sahrani[1], Dayang A. A. Mat[1], and Dyg N. A. Zaidel[1]

Abstract—This paper presents the design of an ultra-wideband (UWB) antipodal Vivaldi antenna (APVA) for radar and microwave imaging applications. A slotted APVA design is introduced to improve the low-end bandwidth limitation frequencies as well as to enhance the gain and directivity of the antenna. The optimizations of the design offer good results by using a cost-effective substrate, fiberglass reinforced grade 4 (FR4) material. The regular APVA antenna design only presents average results of gain (4–6 dBi) and directivity (4–7 dB). However, the addition of slots on the edges of antenna is able to increase the peak value of gain and directivity up to 73.65% with 7.64 dBi and 8.92 dB, respectively. Besides, the radiation pattern of the antenna is also improved by using the slotted design where the main lobe level is larger than regular APVA design. Both antennas presented in this paper are designed in compact size of 42.8 mm × 57.3 mm. The antennas are also designed to operate within the frequency range of 3.6 GHz to 10 GHz frequency.

1. INTRODUCTION

An antenna design being compact, smart, and having multifunctional capabilities has been widely demanded for various applications such as radar, microwave imaging, and remote sensing. To fulfill the industry demand, an ultra-wideband (UWB) antenna is usually the popular types of antenna to use due to its advantages. This antenna has received attention from researchers due to high data rates, low power consumption, and simple hardware configuration in real-life applications [1–3]. However, a huge number of UWB antennas presented in the past focus on omnidirectional radiation patterns with low gain and directivity which is only suitable for short-range communication [4]. For example, in radar applications, a directional antenna with moderate gain is an ideal choice due to its ability of locating the hidden object in walls. Hence, since it was introduced by Gibson [5], tapered slot antenna (TSA) has always been one of the most widely used wideband antennas. In order to meet specific requirement of the industry, TSA grows with various designs such as linear tapered, constant-width tapered, and logarithmically tapered slot antennas [6–10]. This kind of antennas is among the popular choice antennas as it provides wide impedance bandwidth, high gain characteristic, stable radiation patterns [11], and symmetric beam in both E- and H-planes [5, 12]. The TSA with the bandwidth proportional to the length and aperture of the antenna makes it easier to design. Theoretically, TSA has an infinite bandwidth which categorizes it as an endfire travelling wave antenna [13].

An antipodal Vivaldi antenna (APVA) is widely used in applications such as microwave imaging [14], high range radar systems [15], and many other applications that require UWB and end-fire radiation pattern. APVA is one of the TSA family along with conventional Vivaldi antenna and balanced antipodal

Received 12 December 2018, Accepted 23 January 2019, Scheduled 3 April 2019

* Corresponding author: Kismet Anak Hong Ping (hpkismet@unimas.my).

[1] Applied Electromagnetic Research Group, Faculty of Engineering, Universiti Malaysia Sarawak, Kota Samarahan, Sarawak 94300, Malaysia. [2] Department of Computer and Communication Systems Engineering, Universiti Putra Malaysia, UPM Serdang, Selangor 43400, Malaysia.

Vivaldi antenna (BAVA) [14, 15]. In spite of its advantages, this antenna has always been recognized for its simple design [11, 16–18], which only consists of a radiating structure and transmission line (e.g., stripline or microstrip line).

A compact printed APVA with the improvement of rectangular slotted design is proposed in this paper. The modification of a rectangular shape slot is designed for the purpose of redirecting the current density flows from the transmission line to spread at the flare of the antenna. In addition, the improved antenna structure allows the extension of low-end bandwidth limitation frequency of the antenna. Besides, the improvement of the antenna performances is achieved so that the antenna can be applied to radar and microwave imaging application. The design and geometry of the proposed antenna are presented and discussed in detail along with simulated and measured results in the following sections.

2. ANTENNA DESIGN

The proposed antenna is designed on a cost-effective substrate (FR4 substrate) that consists of dielectric constant $\varepsilon_r = 4.4$, dielectric loss tangent $\delta = 0.02$, and thickness $T_S = 1.6\,\text{mm}$. The dimension and parameters of the proposed antenna are illustrated in Figure 1. The design step starts with the selection of the lowest operating frequency for the antenna. Naturally, the lower frequency (f_L) of antenna operation depends on both effective dielectric constant (ε_{eff})) and width (W). However, the upper frequency for the Vivaldi antenna family is infinite. Hence, the lower limit frequency can be calculated by using Equations (1) and (2). The details of parameters can be found in [19, 20]:

$$f_L = \frac{c}{2W\sqrt{\varepsilon_{eff}}} \tag{1}$$

$$\varepsilon_{eff} = \frac{\varepsilon_r + 1}{2} + \frac{\varepsilon_r - 1}{2}\left(1 + \frac{12T_S}{W}\right)^{\frac{1}{2}} \tag{2}$$

The design of the flare aperture of APVA is the crucial part. This is to allow the injected power through the antenna to be successfully transmitted to the receiver. It is used to determine the lobe size of the radiation pattern. The curvature of the flare aperture depends on the shape of the outer edges and inner edges. The estimation of these edges can be found in [5].

$$y = \pm\left(Ae^{R_X} + B\right) \tag{3}$$

where

$$A = \frac{y_2 - y_1}{e^{R_{X_2}} - e^{R_{X_1}}}, \quad B = \frac{y_1 e^{R_{X_2}} - y_2 e^{R_{X_1}}}{e^{R_{X_2}} - e^{R_{X_1}}} \tag{4}$$

The values of each peak and lower point of the curvature of the flare are represented by the coordinate of (x_1, y_1) and (x_2, y_2) of the curvature point. The factor of the exponential of the curve, R, is given by [5].

$$R = \frac{1}{L_a}\ln\left(\frac{W_a}{s_o}\right) \tag{5}$$

where the length of aperture, width of aperture, and slot width at the origin are represented by L_a, W_a, and s_o, respectively.

The size and dimension are chosen to be $42.8\,\text{mm} \times 57.3\,\text{mm}$ for both antennas. The noticeable improvement of the antenna is by designing the slots near the edges for both patches and the ground of antenna. Figure 1 illustrates the design specification of both APVAs designs. Note that the unit of all parameters in this design is in mm. Referring to Figure 1(a), the slots are designed by means of diminishing the current flow at the region [16]. The idea of the slotted antenna outline is inspired by the fractal antenna design [21]. The slots are located on the wing edges as the current distribution observed at the greatest concentration. A set of calculations has been carried out with the largest dimension of $4.1\,\text{mm} \times 1.5\,\text{mm}$ with 90° angle for each slot. Each area of the rectangular slots is then reduced by half of the largest dimension for each slot on both antenna wings. As results, the improvement slotted design has created an enhancement in antenna performances such as return loss, gain, and directivity.

The value of each exponential curve is determined with the opening rate of $a_u = 0.0777\,\text{mm}$ (outer opening rate), $a_L = 0.1555\,\text{mm}$ (inner opening rate), and $a_g = 0.0777\,\text{mm}$ (ground curve). The geometry of the proposed antenna is shown in Figure 1.

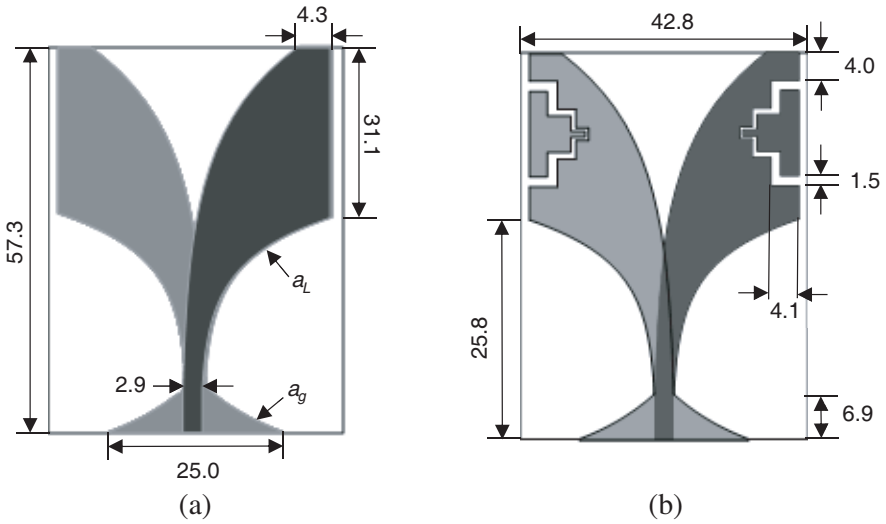

Figure 1. Dimension of proposed antenna. (a) Conventional APVA. (b) Improvement slotted APVA design.

3. RESULTS AND DISCUSSION

Figure 2 illustrates the results of return loss (S_{11}) variation between the conventional APVA and slotted APVA within the operational frequency of 3.6–10 GHz. The lower end of the conventional APVA is noted falling below −10 dB at 4.18 GHz while the slotted APVA is at 3.6 GHz with 13.88% improvement in the result, shown in Figure 2. The starting point of the operating frequency of the antenna below −10 dB is shifted to lower frequency without altering the original antenna size. Consequently, a larger bandwidth of frequency with minimizing the working frequency is achievable by using slotted APVA design. Furthermore, the slotted design is useful in controlling the antenna's bandwidth [22] and introduces the capacitive reactance that reacts with inductive reactance near the transmission line [4].

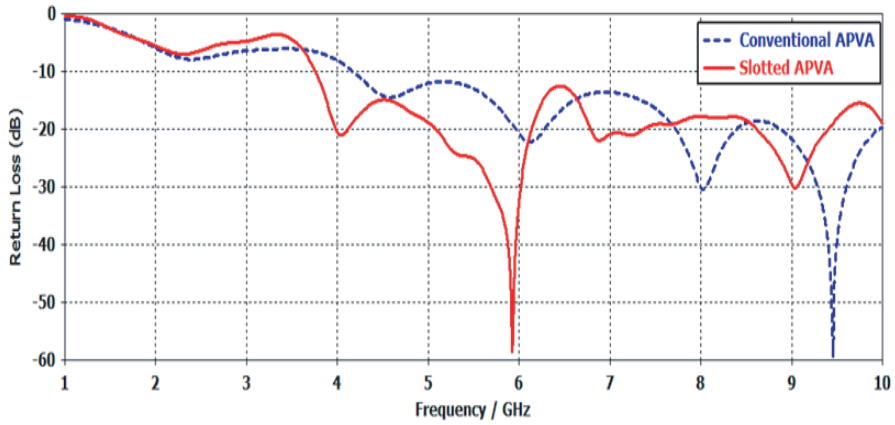

Figure 2. Return loss (S_{11}) results of conventional APVA and slotted APVA design.

Subsequently, a comparison of current density flows (labelled as an elliptical shape) in the antenna at 4 GHz is shown in Figure 3. The behaviour of the current distribution for the conventional APVA antenna as shown in Figure 3(a) is observed to flow in a direction at edges of the wings. The lack of current flow towards the antenna flare has drawn the values of gain and directivity of the antenna. As to address the issues, the rectangular shape slots are designed on the edges of antenna sections as shown in Figure 3(b). The slots have created an effective length of the diversion of current density to flow in

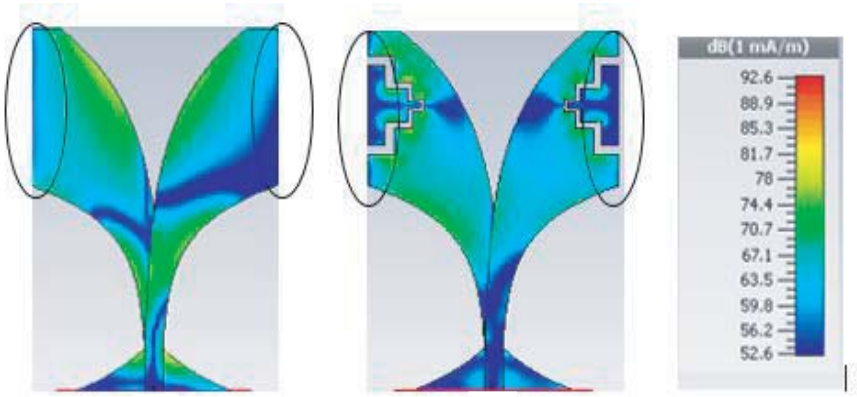

Figure 3. Surface current distribution at 4 GHz frequency. (a) Conventional APVA. (b) Slotted APVA.

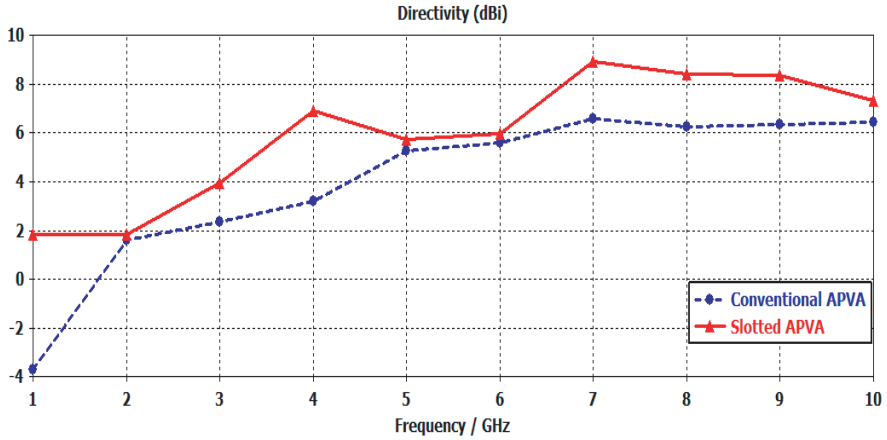

Figure 4. Variation of simulation result of antenna directivity between conventional APVA and slotted APVA.

the direction of the flare and allow the antenna radiated directionally on one area only. Moreover, the changes in the current density distribution have increased the capacitance value, as well as changing the magnetic field distribution of the equivalent inductance value. Referring to conventional design, the patch edges are more likely characterized as the resistor, while the slotted edges are defined as an RLC resonator [23]. Hence, the resonant wavelength of each slot can be estimated as follows,

$$\lambda_O = \frac{4l_s}{\sqrt{\frac{1+\varepsilon_r}{2}}} \tag{6}$$

where l_s refers to the length of the slot, and ε_r is the dielectric of substrate used.

The comparison of the directivities for the two antenna designs is illustrated in Figure 4. In particular, the values of directivity have been improved as slotted design is introduced. The directivity of the antenna reaches the peak value with the reading of 8.92 dBi (slotted APVA) compared to the conventional APVA which only achieves 6.57 dBi at 7 GHz. In addition, the gain of the new design is also improved. Referring to Figure 5, the antenna reaches the maximum gain at 7.64 dB as compared to the conventional APVA at 6.57 dB. An enhancement of 73.65% of the gain affirms that the slotted APVA design is more reliable in performance than similar size conventional APVAs. The improvement in both gain and directivity of the proposed antenna shows that the antenna is able to works efficiently in microwave imaging applications.

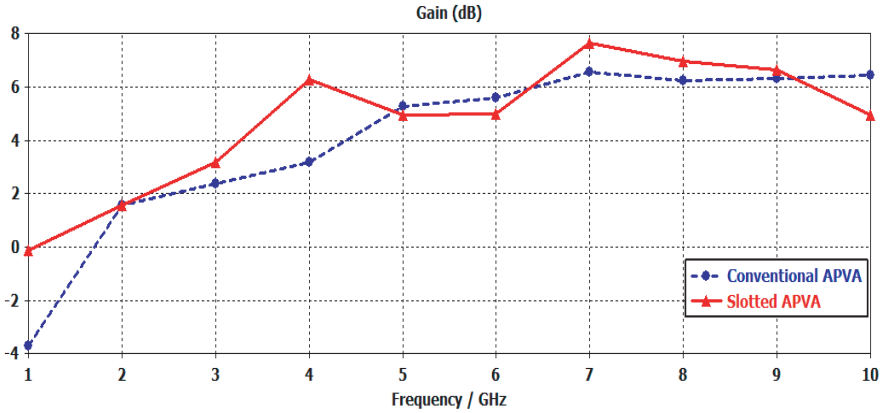

Figure 5. Comparison of gain between conventional APVA and slotted APVA.

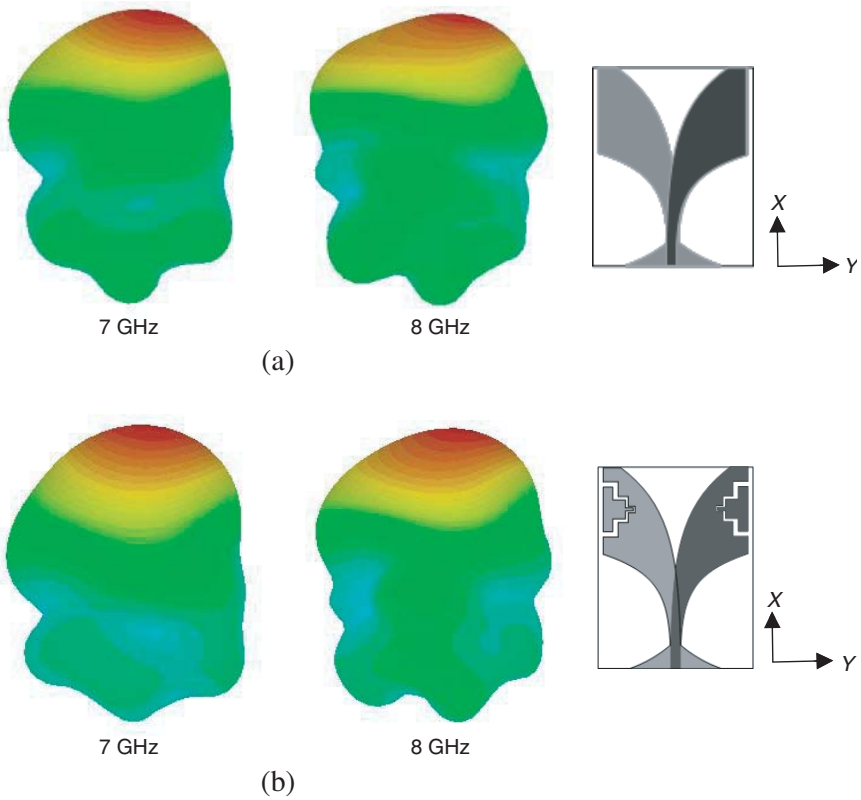

Figure 6. 3-D radiation pattern at selected frequency.

Figure 6 shows 3-D radiation patterns of the proposed antennas at the frequencies of 7 GHz and 8 GHz, respectively. As shown in Figure 6, the 3-D illustration of both antenna designs shows a steady end-fire radiation pattern. The slotted APVA has improved the directional radiation pattern in comparison to the conventional APVA. Based on Figure 6(b) it is observed that the side lobe of the antenna is fixed in the end-fire direction for both frequencies compared to Figure 6(a). Hence, the significant improvement is the main lobe of the radiation pattern. The slotted APVA shows the improvement of low back lobe and side lobe levels and increasing radiating at the bore side as the results of increasing in the gain and directivity values of the antenna. Thus, it has a greater size in terms of coverage of the antenna as compared to the conventional design.

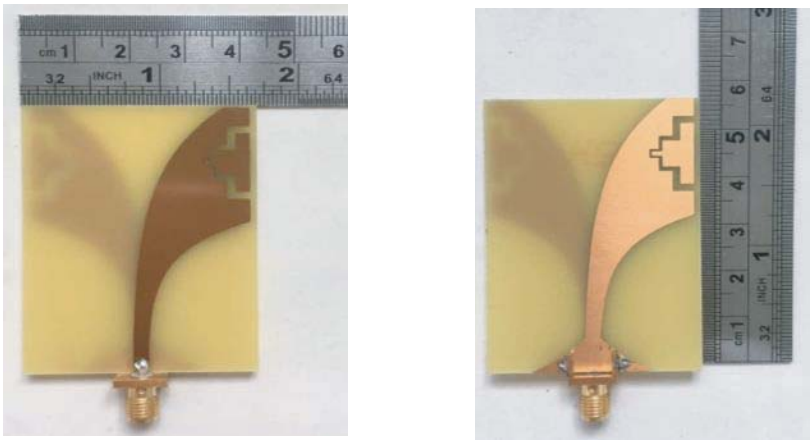

(a) (b)

Figure 7. Fabricated slotted APVA. (a) Front view. (b) Back view.

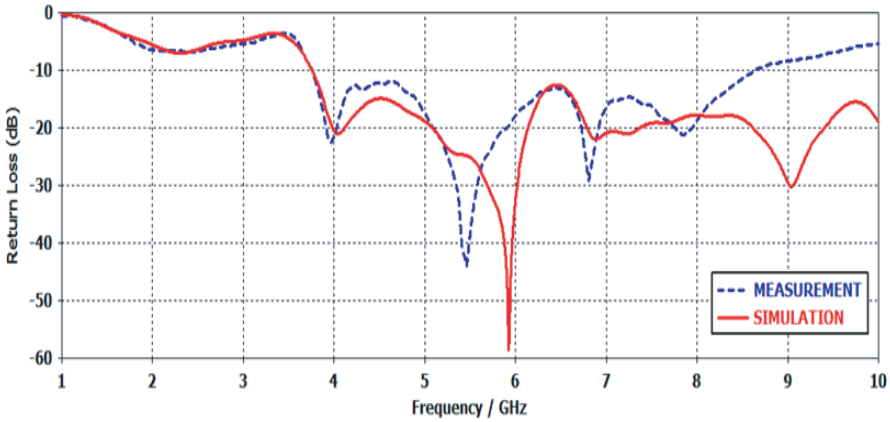

Figure 8. Simulated versus measured results of return loss (dB) against frequency (GHz).

To validate the results, the proposed slotted APVA antenna has been fabricated and measured. The antenna is fabricated on an FR4 board as shown in Figure 7. The contrast of simulation and measurement results of the antenna design involves the performances in S_{11} (return loss) and the radiation pattern of the antenna.

The comparison of return loss results for simulation and measurement is illustrated in Figure 8. The minimum frequency of the antenna falling below -10 dB is similar to the simulated result at the frequency 3.6 GHz. It shows constructive results as the measurement values has no abundant difference from the simulation results. Nevertheless, there is a slightly difference in the operating frequency for simulated and measurement outcomes. Based on Figure 8, it is shown that the operating frequency of the measured antenna falls on 5.9 GHz (with -58.29 dB return loss) which is shifted by 0.45 GHz from the simulation value. Besides, the return loss of the antenna falling below -10 dB is limited to 8.8 GHz while the simulation results continue to be under -10 dB throughout the 10 GHz frequency. In such a way, the difference in values between the two antennas is caused by the discontinuity in the feedline [16, 21] and fabrication tolerances. The main factor of the discontinuity comprises overheat while attaching the SMA port onto the antenna as well as the effect of dielectric loss during the process of fabrication. Overall, the comparison of the return losses between the simulated and measured slotted APVAs shows a good result to operate for radar and microwave imaging applications.

Figure 9 illustrates the results of simulation and measurement radiation patterns at 5, 6, 7, and 8 GHz, respectively. The presentation of the results consists of 2 parts labeled as E-plane and H-plane.

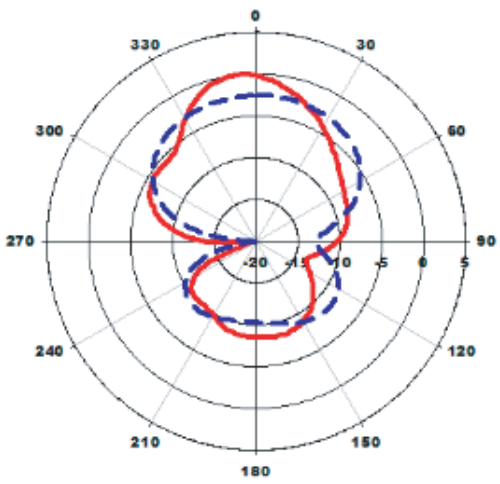

(*E*-Plane)

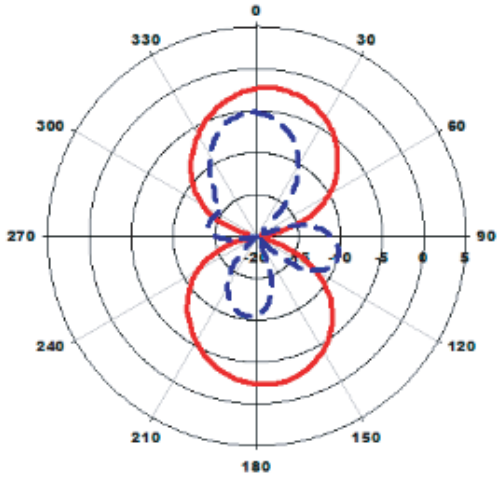

(*H*-Plane)

(a) 5 GHz

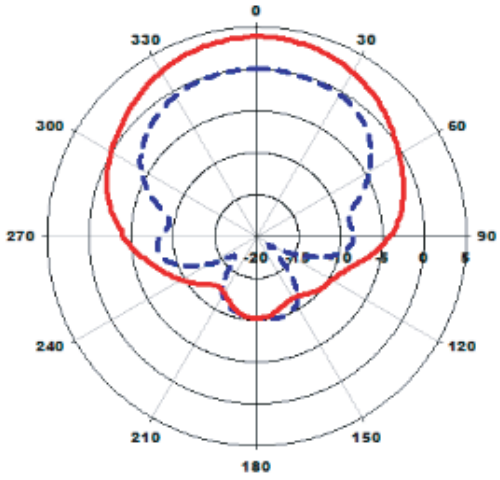

(*E*-Plane)

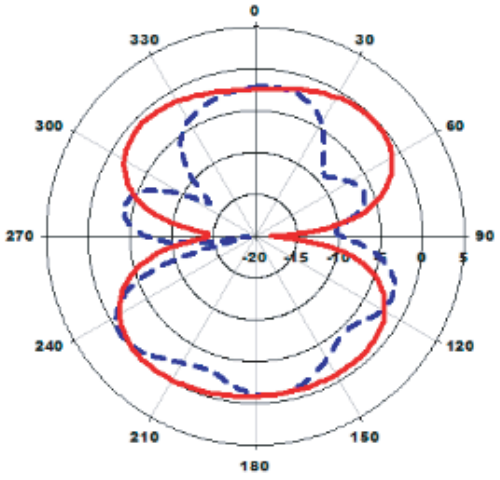

(*H*-Plane)

(b) 6 GHz

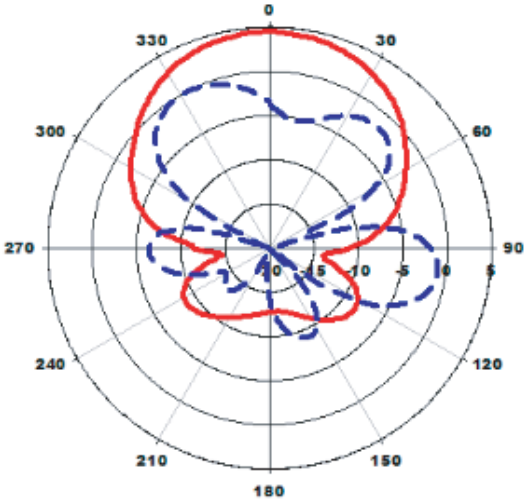

(*E*-Plane)

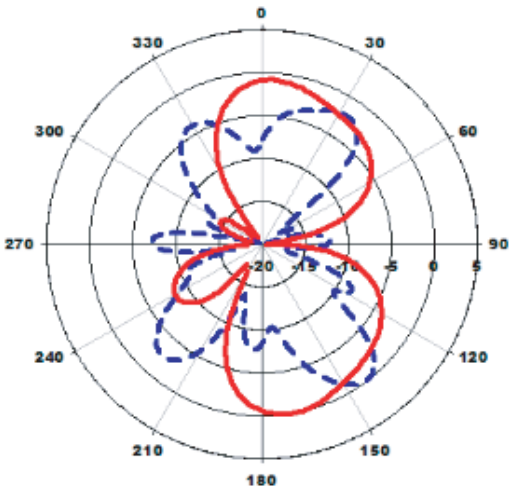

(*H*-Plane)

(c) 7 GHz

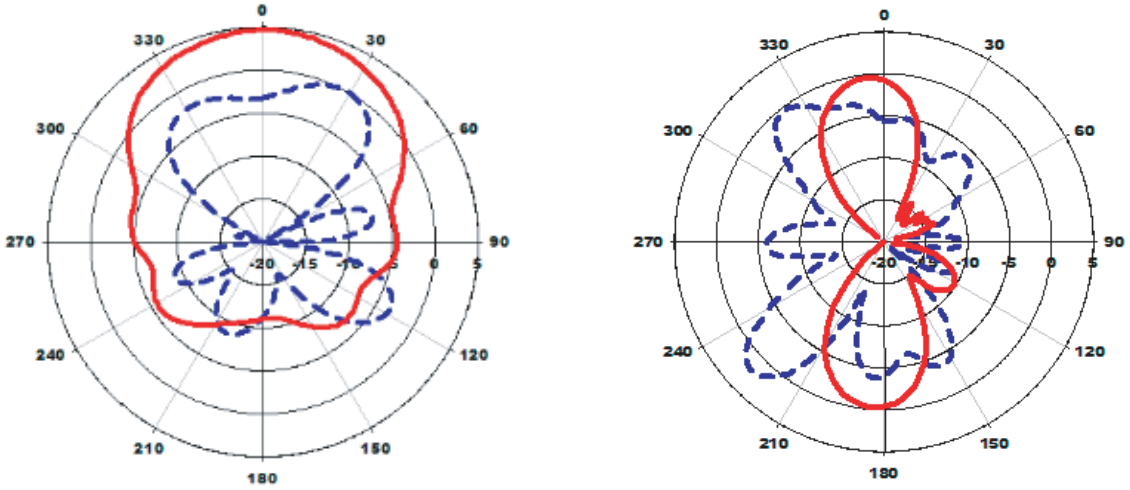

(d) 8 GHz

Figure 9. Simulated (—) radiation patterns against measured (−−) at E-Plane and H-Plane at selected frequency.

The radiation pattern of the slotted APVA shows a directional pattern of frequency listed. The location of the main lobe describes the concentration of the fields of the radiation focussing at the patch area of the antenna. On the contrary, the radiation pattern is curbed at angles 90° and 270°, denoting the patch and ground of the slotted APVA. The increase in frequency shows that more lobes are mapped in the radiation pattern. The larger size lobes are related to the concentration of the fields which is gradually increased as the current flows is increased in the direction of the flare aperture of the antenna. Thus, the results of main lobe show the progression of antenna performances in terms of both gain and directivity.

4. CONCLUSION

A UWB antenna with slotted design with improved performances has been designed. With the compact antenna design (42.75 mm × 57.25 mm), the antenna provides a wideband matching with a good return loss within the operating frequency up to 10 GHz. Thus, the slotted design on the antenna allows the return loss result to fall under −10 dB at 3.6 GHz as compared to the conventional design. The new design has shown a significant improvement in terms of return loss, gain, directivity, and radiation pattern. Therefore, the slotted APVA design is proven to be better in performance than the conventional APVA design. The proposed antenna is suitable to be used for high range radar applications with design in arrays and a suitable candiate for microwave imaging applications.

ACKNOWLEDGMENT

The authors gratefully acknowledge Universiti Malaysia Sarawak (UNIMAS) and Universiti Kebangsaan Malaysia (UKM) for the support in obtaining the information and materials in the development of our works.

REFERENCES

1. George, T., "Ultra-wideband and applications," *SCMS School of Engineering and Technology*, 2014, [online], available: https://www.slideshare.net/thomasgeorgec/uwb-and-applications, [accessed: 20-Jul.-2017].

2. Rahman, A., M. T. Islam, M. J. Singh, S. Kibria, and M. Akhtaruzzaman, "Electromagnetic performances analysis of an ultra-wideband and flexible material antenna in microwave breast imaging: To implement a wearable medical bra," *Sci. Rep.*, Vol. 6, 1–11, Dec. 2016.
3. Herzi, R., H. Zairi, and A. Gharsallah, "Antipodal Vivaldi antenna array with high gain and reduced mutual coupling for UWB applications," *2015 16th International Conference on Sciences and Techniques of Automatic Control and Computer Engineering (STA)*, 789–792, 2015.
4. Mobashsher, A. and A. Abbosh, "Utilizing symmetry of planar ultra-wideband antennas for size reduction and enhanced performance," *IEEE Antennas Propag. Mag.*, 1–27, 2015.
5. Gibson, P. J., "The Vivaldi aerial," *9th European Microwave Conference, 1979*, 101–105, 1979.
6. De Lera Acedo, E., E. García, V. González-Posadas, J. L. Vázquez-Roy, R. Maaskant, and D. Segovia, "Study and design of a differentially-fed tapered slot antenna array," *IEEE Trans. Antennas Propag.*, Vol. 58, No. 1, 68–78, 2010.
7. Brenda, "Vivaldi antenna," *Microwaves101.com*, 2013, [online], available: https://www.microwaves101.com/encyclopedias/vivaldi-antenna, [accessed: 04-Oct.-2017].
8. Yim, T. L., S. K. A. Rahim, and R. Dewan, "Reconfigurable wideband and narrowband tapered slot Vivaldi antenna with ring slot pairs," *Journal of Electromagnetic Waves and Applications*, Vol. 27, No. 3, 276–287, 2013.
9. Li, Y., S. Lin, J. Chen, and J. Ou, "Design of a wideband dual-polarized linearly tapered slot antenna," *2011 International Conference on Electronics, Communications and Control, ICECC 2011 — Proceedings*, 210–213, 2011.
10. Yao, Y., W. Chen, B. Huang, Z. Feng, and Z. Zhang, "Analysis and design of tapered slot antenna for ultra-wideband applications," *Tsinghua Sci. Technol.*, Vol. 14, No. 1, 1–6, 2009.
11. Pandey, G. K., H. S. Singh, P. K. Bharti, A. Pandey, and M. K. Meshram, "High gain Vivaldi antenna for radar and microwave imaging applications," *Int. J. Signal Process. Syst.*, Vol. 3, No. 1, 35–39, 2014.
12. Wolff, C., "Tapered slot antenna (Vivaldi antenna)," *Christian Wolff*, 2013, [online], available: http://www.radartutorial.eu/06.antennas/Tapered Slot Antenna.en.html#this, [accessed: 05-Oct.-2017].
13. Fei, P., Y. C. Jiao, W. Hu, and F. S. Zhang, "A miniaturized antipodal vivaldi antenna with improved radiation characteristics," *IEEE Antennas Wirel. Propag. Lett.*, Vol. 10, 127–130, 2011.
14. Alzabidi, M. A., M. A. Aldhaeebi, and I. Elshafiey, "Development of UWB Vivaldi antenna for microwave imaging," *2013 Saudi International Electronics, Communications and Photonics Conference, SIECPC 2013*, 2013.
15. Maalik, S., "Antenna design for UWB radar detection application," *Antenna*, 2010.
16. Kang, X. and Z. Li, "A modified UWB antipodal Vivaldi antenna with improved radiation characteristics," *2015 IEEE 6th International Symposium on Microwave, Antenna, Propagation, and EMC Technologies (MAPE)*, Vol. 2, No. 1, 120–122, 2015.
17. Fisher, J., "Design and performance analysis of a 1–40 GHz ultra-wideband antipodal Vivaldi antenna," *Proc. Ger. Radar Symp. GRS*, Vol. 6002, 2000.
18. Gazit, E., "Improved design of the Vivaldi antenna," *IEE Proc. H, Microwaves, Antennas Propag.*, Vol. 135, No. 2, 89–92, 1988.
19. Wang, S., X. D. Chen, and C. G. Parini, "Analysis of ultra wideband antipodal Vivaldi antenna design," *Proc. of 2007 Loughbrgh. Antennas Propag. Conf., LAPC*, Vol. 0, 129–132, Apr. 2007.
20. Balanis, C. E., *Antenna Theory: Analysis and Design*, 3rd edition, 1136, Wiley Interscience, 2005.
21. Yu, Y. and C. Ji, "Research of fractal technology in the design of multi-frequency antenna," *2011 China-Japan Jt. Microw. Conf.*, 1–4, 2011.
22. Chen, W. L., G. M. Wang, and C. X. Zhang, "Bandwidth enhancement of a microstrip-line-fed printed wide-slot antenna with a fractal-shaped slot," *IEEE Trans. Antennas Propag.*, Vol. 57, No. 7, 2176–2179, 2009.
23. Bai, J., S. Shi, and D. W. Prather, "Modified compact antipodal Vivaldi antenna for 4–50-GHz UWB application," *IEEE Trans. Microw. Theory Tech.*, Vol. 59, No. 4, Part 2, 1051–1057, 2011.